mTORC1 is a key regulator that mediates OGD- and TGFβ1-induced myofibroblast transformation and chondroitin-4-sulfate expression in cardiac fibroblasts

CHAO LI[1,2], ZHENG ZHANG[1,3], YU PENG[2,3], YANYING ZHANG[4],
WANRONG KANG[4], YINGDONG LI[5] and YANG HAI[4]

[1]The First Clinical College, Lanzhou University; [2]Gansu Key Laboratory of Cardiovascular Disease,
The First Hospital of Lanzhou University; [3]Department of Cardiology, The First Hospital of Lanzhou University;
[4]Research Experiment Center, Gansu University of Chinese Medicine; [5]Key Laboratory of Prevention and
Treatment for Chronic Disease, Traditional Chinese Medicine of Gansu Province,
Gansu University of Chinese Medicine, Lanzhou, Gansu 730000, P.R. China

Abstract. Ischemia-reperfusion infarct-derived chondroitin sulfate proteoglycans (CSPGs) are important for sustaining denervation of the infarct. Sympathetic denervation within the heart after myocardial infarction (MI) predicts the probability of a higher risk for serious ventricular arrhythmias. Chondroitin-4-sulfate (C4S) is the predominant chondroitin sulfate component in the heart. However, the mechanisms that induce CSPG expression in fibroblasts following MI remain to be elucidated. The present study found that oxygen-glucose deprivation (OGD) and TGFβ1 stimulation induced myofibroblast transformation and C4S synthesis *in vitro* by using reverse transcription-quantitative PCR, western blotting and immunofluorescence. MTT assay was used to detect cell viability following OGD or OGD + TGF lotreatment. Using the PI3K inhibitor ZSTK474, the Akt inhibitor MK2206, or the mTOR inhibitor AZD8055, it was observed that OGD and TGFβ1 stimulation induced myofibroblast transformation and that C4S synthesis was mTOR-dependent, whereas the upstream canonical PI3K/Akt axis was dispensable by using western blotting and immunofluorescence. siRNA knockdown of Smad3, Raptor, or Rictor, indicated that mTORC1 was critical for promoting OGD- and TGFβ1-induced myofibroblast transformation and C4S synthesis by using western blotting and immunofluorescence. This response, may be mediated via cooperation between canonical Smad3 and mTORC1 signaling. These data suggested that inhibiting myofibroblast transformation may reduce C4S synthesis. Target mTORC1 may provide additional insight into the regeneration of sympathetic nerves and the reduction of fibrosis after MI at the cellular level. These findings may contribute to the understanding of the mechanism by which C4S overproduction in the hearts of patients with MI is associated with myocardial fibrosis.

Introduction

Acute myocardial infarction (AMI) is a leading cause of mortality worldwide. Although the current effective percutaneous coronary intervention and thrombolytic therapy have saved the lives of countless patients, ischemia and reperfusion (I/R) injury can also cause further damage to the heart (1,2). Following MI, TGFβ1 is markedly upregulated, inducing fibroblast activation and cell phenotypic conversion from fibroblasts to myofibroblasts. Myofibroblasts express α-smooth muscle actin (α-SMA) and secrete large amounts of extracellular matrix (ECM) proteins (3). Following MI injury the accumulation of ECM is critical for acute wound healing; however, in response to myocardial injury, persistent fibroblast activation and cell phenotypic conversion from fibroblasts to myofibroblasts result in the excessive production and accumulation of ECM proteins and excessive fibrosis worsens disease and accelerates the progression to heart failure (HF) (4).

ECM contains structural components such as collagen and nonstructural components, including glycoproteins, proteoglycans and glycosaminoglycans (5). Chondroitin sulfate proteoglycans (CSPGs) consist of core proteins with covalently attached chondroitin sulfate (CS) chains (6). CS is a class of sulfated glycosaminoglycan chains composed of a repeating disaccharide unit consisting of glucuronic acid (GlcA) and *N*-acetylgalactosamine (GalNAc). Biosynthesis of CS is initiated by addition of the linkage tetrasaccharide sequence to a specific serine residue in a core protein (7). The sulfation pattern of CS is known to be important for the

Correspondence to: Professor Zheng Zhang, Department of Cardiology, The First Hospital of Lanzhou University, 1 Donggang West Road, Lanzhou, Gansu 730000, P.R. China
E-mail: zhangccu@163.com

specific functions of CS. CSPGs that promote fibrogenesis are deposited in the fibrosis model induced by bleomycin (8). A previous study demonstrated that excessive CSPG deposition is associated with impaired cardiac function with ischemic HF in animal models and patients (9). Another study confirmed that TGFβ induces chondroitin-4-sulfate (C4S) upregulation in cardiac fibroblasts (CFs) and found that C4S also accumulates in fibrotic regions of the pathologically remodeled left ventricle (LV) (5). However, the mechanisms that induce CSPG expression in fibroblasts following MI remain to be elucidated.

A previous study confirmed that I/R infarct-derived CSPGs are important for sustaining denervation of the infarct (10,11). Another study demonstrated that CSPGs accumulate in the ECM of the injured central nervous system (CNS) and are synthesized by reactive astrocytes, limiting axonal regeneration (12). TGFβ1 signals through the canonical Smad pathway and several noncanonical pathways affect cell function (13). A previous study on CNS injury confirmed that TGFβ-Smad3 mediates astrocyte-secreted 4-sulfation (14). However, another study reported that TGFβ mediates CSPG expression through non-Smad-mediated activation of the PI3K-Akt-mTOR signaling pathway (15). Notably, a previous study demonstrated that canonical PI3K/Akt signaling has no effect on TGFβ1-induced collagen deposition in pulmonary fibroblasts and this response may be mediated via cooperation between canonical Smad3 and mTORC1 signaling (13). Therefore, the purpose of the present study was to examine whether oxygen-glucose deprivation (OGD) and TGFβ1 stimulation induced myofibroblast transformation and CSPG synthesis in fibroblasts mediated by cooperation between canonical Smad3 and mTORC1 signaling.

Materials and methods

Primary cell isolation, culture and in vitro treatment. Adult rat ventricular CFs were isolated as previously described (16). In brief, a total of 48 adult male Sprague-Dawley rats (age, 8- to 10-week-old; weight, 150-200 g) were provided by the Laboratory Animal Centre of the Gansu University of Chinese Medicine. All experimental subjects were maintained in a specific pathogen-free grade environment at a temperature of $23\pm2°C$ with a humidity of 50-60%, a 12-h light/dark cycle and free access to food and water. The rats were anaesthetized via intraperitoneal injection of 3% sodium pentobarbital (30 mg/kg). Hearts were then excised from anesthetized rats and rinsed in cold phosphate-buffered saline. The ventricles were cut into pieces of ~1 mm³ in Dulbecco's modified Eagle's medium (DMEM; Gibco; Thermo Fisher Scientific, Inc.), digested in 0.25% trypsin (Dalian Meilun Biotechnology Co., Ltd.) and subsequently digested in DMEM containing 0.1% collagenase type II (MilliporeSigma). The cells were collected and cultured in DMEM containing 10% fetal calf serum, 100 U/ml penicillin (Dalian Meilun Biotechnology Co., Ltd.) and 100 mg/ml streptomycin (Dalian Meilun Biotechnology Co., Ltd.) at 37°C and 5% CO_2 for 1 h. After pre-plating, the adherent cells were cultured. The purity of CFs was >95%, as determined by positive staining for vimentin. Cells at passage 1 were used in the present study. All experimental procedures were performed in accordance with the Guide for the Care

and Use of Laboratory Animals published by the National Research Council and were approved by the Animal Care Committee of the Gansu University of Chinese Medicine (approval number 2019-212).

Cultured cells subjected to hypoxia and fuel deprivation provide an efficient *in vitro* model to examine the cellular mechanisms mediating ischemic injury (17). Cells were cultured to 70-80% confluence, at which point the medium was changed to serum- and glucose-free DMEM (Dalian Meilun Biotechnology Co., Ltd.). Cells were transferred into a triple gas incubator with hypoxic (5% CO_2, 1% O_2 and 94% N_2) settings and incubated under hypoxic conditions and flushed with the same gas mixture. After exposure to OGD for 12 h, the cells were placed under normal conditions (DMEM containing serum and glucose) for reoxygenation for 24 h for RNA detection or 48 h for protein detection. During reoxygenation, the treated groups were stimulated with TGFβ1 (10 ng/ml; PeproTech, Inc.). The corresponding control cells were incubated in DMEM containing serum and glucose under normoxic conditions for equivalent durations.

Pharmacological inhibitors. The contribution of the PI3K/Akt/mTOR signaling axis to OGD- and TGFβ1 stimulation-induced myofibroblast transformation and CSPG synthesis was investigated by evaluating the effect of highly selective inhibitors of critical components of the PI3K/Akt/mTOR axis: PI3K (cat. no. ZSTK474; MedChem Express), Akt (cat. no. MK2206; MedChem Express) and mTOR (cat. no. AZD8055; MedChem Express). Stock solutions of ZSTK474 (1 mM), MK2206 (1 mM) and AZD8055 (1 mM) were prepared. All chemicals were prepared in dimethyl sulfoxide (DMSO; Beijing Solarbio Science & Technology Co., Ltd.).

All groups except the control group received one of the following treatments: ZSTK474 (1 μM, 100 nM, 10 nM or 1 nM), MK2206 (1 μM, 100 nM, 10 nM or 1 nM), AZD8055 (1 μM, 100 nM, 10 nM or 1 nM) for 4 h before exposure to OGD + TGFβ1. The inhibitor concentration was always consistent in subsequent processing.

Cell viability by the 3-(4,5-dimethylthiazol-2-yl)-2,5-di-phenyl-2H-tetrazolium bromide (MTT) assay. CFs were seeded in 96-well plates (density; 1x10⁴ cells/well) in DMEM media and were stimulated under the conditions indicated for each experiment. Cell viability was measured using the MTT assay (Beijing Solarbio Science & Technology Co., Ltd.). Briefly, MTT solution (final concentration, 0.5 mg/ml) was added to each well and the cells were incubated at 37°C for 4 h. Culture supernatant was then removed and 110 μl DMSO was added to each well to dissolve formazan crystals and the absorbance at 490 nm was measured by using an infinite M200PRO microplate reader (Tecan Group, Ltd.). Data from 3 independent experiments were used for analysis.

Short interfering (si)RNA transfection. For siRNA knockdown experiments, rat-specific Smad3 siRNA, Raptor siRNA, Rictor siRNA and negative control siRNA were purchased from Shanghai GenePharma Co., Ltd. The siRNA was diluted in serum-free media and rat CFs were either transfected with Smad3 siRNA (10 nM), Raptor siRNA (10 nM), Rictor siRNA (10 nM) or negative control siRNA (10 nM) using

Lipofectamine® RNAi/MAX Reagent (Invitrogen; Thermo Fisher Scientific, Inc.) at 37°C for 48 h according to the manufacturer's protocols, after which the cells were harvested for western blotting analysis to evaluate the specific silencing effect of siRNA. Following transfection, the cells were used for subsequent experiments. The sequences of the Smad3 siRNA were sense 5'-GAUCGAGCUACACCUGAAUTT-3' and antisense 5'- AUUCAGGUGUAGCUCGAUCTT-3'. The sequences of the Raptor siRNA were sense 5'-GUGGCAAGU UUGUUUAGAATT-3' and antisense 5'-UUCUAAACAAAC UUGCCACTT-3'. The sequences of the Rictor siRNA were sense 5'-GCAGCCCUGAACUGUUUAATT-3' and antisense 5'-UUAAACAGUUCAGGGCUGCTT-3'. The sequences of the negative control siRNA were sense 5'-UUCUCCGAACGU GUCACGUTT-3' and antisense 5'-ACGUGACACGUUCGG AGAATT-3'.

RNA extraction and reverse transcription-quantitative (RT-q) PCR. Total RNA ($5x10^6$ cells) was extracted using TRIzol® reagent (Thermo Fisher Scientific, Inc.) according to the manufacturer's instructions. RNA was subsequently reverse transcribed using PrimeScript RT Master Mix (Takara Biotechnology Co., Ltd.). The reaction temperature of reverse transcription was 37°C for 15 min and 85°C for 5 sec. RT-qPCR was performed using SYBR Premix Ex Taq II (Takara Biotechnology Co., Ltd.). All reaction were performed with the following cycling parameters: 95°C for 30 sec, followed by 40 cycles of 95°C for 5 sec, 60°C for 34 sec and a final stage of 95°C for 15 sec, 60°C for 60 sec and 95°C for 15 sec. Relative expression of all genes was calculated by normalizing to the levels of expression of the internal reference gene β-actin using the $2^{-\Delta\Delta Cq}$ method (18). Data from 3 independent experiments were used for analysis of relative gene expression. A list of the genes and primers used is provided in Table SI.

Sample preparation and western blotting
CFs conditioned media. CF-conditioned medium was placed into a tube containing complete protease inhibitors (Roche Diagnostics). The conditioned medium was then centrifuged at 4,000 x g at 4°C for 20 min to concentrate using an Amicon Ultra-15 NMWL100K centrifugal filter device (MilliporeSigma). The protein concentration was measured using a BCA protein assay reagent (Beijing Solarbio Science & Technology Co., Ltd.). Protein ($30 \mu g$) was loaded onto 8% gels, subjected to SDS-PAGE and then transferred to PVDF membranes (MilliporeSigma). Following blocking with 5% skimmed milk at room temperature for 1 h, membranes were incubated with the following primary antibody: anti-2H6 (Cosmo Bio) at 4°C overnight. The secondary antibody was horseradish peroxidase (HRP)-conjugated anti-mouse IgG (ImmunoWay Biotechnology Company) and was incubated with the membranes at room temperature for 1 h. Proteins were visualized using Enhanced Chemiluminescence (ECL) western blotting Substrate (Dalian Meilun Biotechnology Co., Ltd.) and gel images were visualized using a Universal Hood II (Bio-Rad Laboratories, Inc.) and quantified using ImageJ 1.51k software (NIH). Catalog numbers and dilutions of antibodies are provided in Table SII.

Cell lysates. CFs were lysed in RIPA buffer containing 1% phenyl-methylsulfonyl fluoride (Dalian Meilun Biotechnology Co., Ltd.)

and 1% phosphatase inhibitor cocktail (Beijing Solarbio Science & Technology Co., Ltd.). Protein concentration was measured using a BCA protein assay reagent (Beijing Solarbio Science & Technology Co., Ltd.). Protein ($20 \mu g$) was loaded onto 10% gels for SDS-PAGE and then transferred to PVDF membranes (MilliporeSigma). Following blocking with 5% skimmed milk at room temperature for 1 h, membranes were incubated with the following primary antibodies: anti-α-SMA (Abcam), anti-Akt (Cell Signaling Technology, Inc.), anti-phospho-Akt(Ser473) (Cell Signaling Technology, Inc.), anti-PRAS40 (Cell Signaling Technology, Inc.), anti-phospho-PRAS40(Thr246) (Cell Signaling Technology, Inc.), anti-p70S6k (Cell Signaling Technology, Inc.), anti- phospho-p70S6k(Thr389) (Cell Signaling Technology, Inc.), anti-Smad3 (Cell Signaling Technology, Inc.), anti-phospho-Smad3(Ser425) (Affinity), anti-Raptor (Cell Signaling Technology, Inc.), anti-Rictor (Cell Signaling Technology, Inc.) and anti-β-actin (ImmunoWay Biotechnology Company) at 4°C overnight. Secondary antibodies were HRP-conjugated anti-mouse IgG and HRP-conjugated anti-rabbit IgG (ImmunoWay Biotechnology Company) at room temperature for 1 h. Proteins were visualized with ECL western blotting Substrate (Dalian Meilun Biotechnology Co., Ltd.) and gel images were visualized using Universal Hood II (Bio-Rad Laboratories, Inc.) and quantified using ImageJ 1.51k software (NIH). Catalog numbers and dilutions of primary antibodies are provided in Table SII.

Immunofluorescence imaging. Following the aforementioned treatments, cells were fixed in 4% paraformaldehyde for 15 min at room temperature and rinsed with phosphate-buffered saline-(0.05%) Tween 20 (PBST). Cells were then permeabilized using 0.25% Triton X-100 in PBS for 10 min. Next, cells were blocked in 1% bovine serum albumin for 30 min at room temperature. Subsequently, the cells were incubated with primary antibodies against vimentin (Abcam) and α-SMA (Abcam) overnight at 4°C. Cells were then washed with PBST and incubated with Alexa Fluor 594-conjugated goat anti-rabbit secondary antibody (ImmunoWay Biotechnology Company) or Alexa Fluor 488-conjugated goat anti-rabbit/mouse secondary antibody (ImmunoWay Biotechnology Company) for 1 h at room temperature. Stained slides were then rinsed and the coverslips were mounted using prolonged gold anti-fade with DAPI (Beijing Solarbio Science & Technology Co., Ltd.). Fluorescent images of labeled cells in three randomly selected views were captured using an Olympus fluorescence microscope (Olympus Corporation; magnification, x10). Catalog numbers and dilutions of primary antibodies are provided in Table SII.

Statistical analysis. GraphPad Prism 6.0 (GraphPad Software, Inc.) was used for all statistical analyses. Data are expressed as means ± standard deviation. Data were analyzed by unpaired Student's t-tests for studies that had 2 groups and one-way ANOVA with the Bonferroni post hoc test was used to compare 3 or more groups. $P < 0.05$ was considered to indicate a statistically significant difference.

Results

OGD and TGFβ1 induce CF to myofibroblast differentiation and secretion of CSPGs. The purity of CFs was >95%,
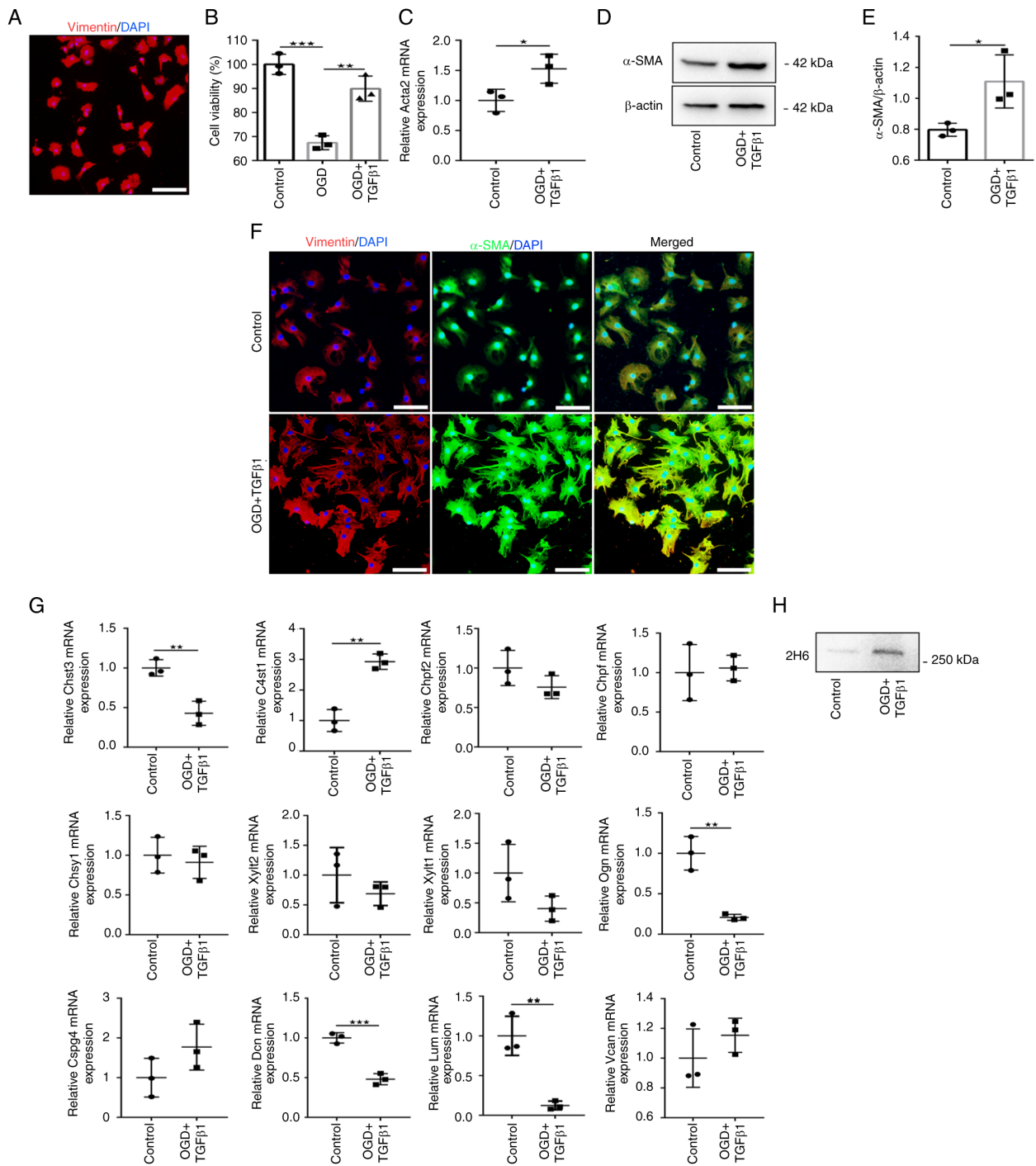
Figure 1. OGD and TGFβ1 induce CF-to-myofibroblast differentiation and secretion of C4S. (A) CFs were identified by positive staining for vimentin (red). Nuclei are stained with DAPI (blue). Scale bar=100 μm. (B) MTT assay detected the cell viability of CFs. (C) Expression levels of Acta2 were detected by reverse transcription-quantitative PCR in the control and OGD + TGFβ1 stimulation groups. Expression levels of α-SMA were (D) detected by western blotting and (E) analyzed. Data are representative of three independent experiments. (F) Representative immunocytochemistry for vimentin (red) and α-SMA (green) in the control and OGD + TGFβ1 treated groups. Nuclei were stained using DAPI (blue). Scale bar=100 μm. (G) Expression of genes related to CSPG protein cores, enzymes for GAG chain initiation and CS chain elongation and sulfotransferases. (H) Expression levels of 2H6 were detected by western blotting in the control and OGD + TGFβ1 treated groups using conditioned media collected from CFs. Data are representative of four independent experiments. [*]P<0.05, [**]P<0.01 and [***]P<0.001. OGD, oxygen-glucose deprivation; CFs, cardiac fibroblasts; α-SMA, α-smooth muscle actin.

as determined by positive staining for vimentin (Fig. 1A). As depicted in Fig. 1B, OGD treatment significantly decreased the cell viability of CF compared with control cells. TGFβ1 addition during reperfusion stimulated showed a significant protection in the loss of CF viability. Treatment of CFs with OGD and TGFβ1 stimulation (treatment group) induced

significant upregulation of the mRNA and protein expression of the myofibroblast marker α-SMA (encoded by Acta2) compared with the control group (Fig. 1C-E). In the treatment group, immunofluorescence staining revealed that the expression of α-SMA was co-labeled with vimentin and cells displayed visible signs of hypertrophy (Fig. 1F). These results
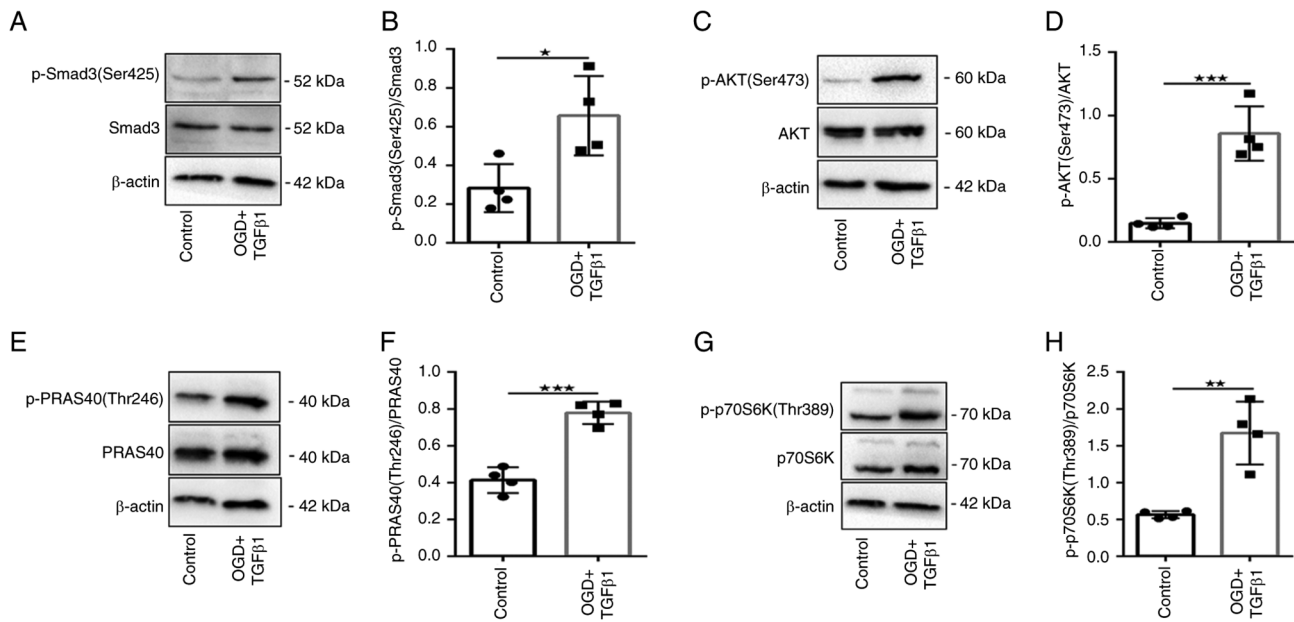
Figure 2. OGD and TGFβ1 induce Smad3 and PI3K/Akt/mTOR signaling in CFs. OGD + TGFβ1 induced phosphorylation of (A and B) Smad3, (C and D) Akt, (E and F) PRAS40 and (G and H) p70S6K was detected by western blotting and analyzed. Data are representative of four independent experiments. *P<0.05, **P<0.01 and ***P<0.001. OGD, oxygen-glucose deprivation; CFs, cardiac fibroblasts; p-, phosphorylated.

demonstrated that OGD and TGFβ1 stimulation induce fibroblast differentiation into myofibroblasts.

CSPG expression in the control and treatment groups were next analyzed (Fig. 1G). The mRNA expression of CSPG protein cores, sulfated glycosaminoglycan (GAG) chain initiation and elongation enzymes and CS sulfatase enzymes were profiled. Among these genes, only C4st1, the C4S sulfotransferase gene, was significantly increased in the treatment group compared with the control group. The expression of other genes revealed that Chst3 (also called C6st1, the C6S sulfotransferase gene), Ogn, Dcn and Lum mRNA levels were significantly decreased in the treatment group. However, expression of all other genes was not altered in response to stimulation. It was confirmed that 2H6 levels, which probe for the major CS component of C4S, using conditioned media collected from CFs, were highly expressed in the treatment group compared with the control group (Fig. 1H). These results demonstrated that fibroblast differentiation into myofibroblasts increases the secretion of C4S.

OGD and TGFβ1 induce Smad3 and PI3K/Akt/mTOR signaling in CFs. As Smad signaling is rapid and relatively short-lived (13), the phosphorylation of Smad3 (Ser425) 2 h after TGFβ1 treatment was detected. The data revealed that Smad3 (Ser425) phosphorylation was significantly increased in the treatment group compared with the control group (Fig. 2A and B).

The phosphorylation of several key targets of the PI3K/Akt/mTOR signaling pathway were next tested: Akt (Ser473), PRAS40 (Thr246) and p70S6K (Thr389). Phosphorylation of Akt (Ser473), PRAS40 (Thr246) and p70S6K (Thr389) was significantly increased in the treatment group compared with the control group (Fig. 2C-H). These data confirmed that CF treatment with OGD and TGFβ1 induces Smad3 and PI3K/Akt/mTOR signaling activation.

The effect of PI3K/Akt/mTOR pathway inhibition on induced myofibroblast transformation and secreted C4S. The role of the PI3K/Akt/mTOR signaling axis in OGD- and TGFβ1-induced myofibroblast transformation and C4S secretion were next investigated. Therefore, the effect of highly selective inhibitors of critical components of the PI3K/Akt/mTOR axis were examined: PI3K (ZSTK474), Akt (MK2206) and mTOR (AZD8055). ZSTK474 reduced Akt Ser473 phosphorylation and inhibited the phosphorylation of PRAS40 Thr246, a downstream substrate of Akt (Fig. 3A-C). By contrast, treatment of fibroblasts with 1 μM ZSTK474 had no effect on the protein expression of α-SMA or 2H6 compared with DMSO-treated fibroblasts that received OGD and TGFβ1 stimulation (Fig. 3D-F). Similarly, fibroblasts treated with MK2206 exhibited robust attenuation of Akt Ser473 and PRAS40 Thr246 phosphorylation (Fig. 4A-C), but fibroblasts treated with 1 μM MK2206 exhibited no effects on protein expression of α-SMA or 2H6 (Fig. 4D-F). Fluorescence immunohistochemistry for α-SMA was then performed and fibroblasts retained a reactive phenotype in the presence of 1 μM ZSTK474 or MK2206 (Fig. 5). These results suggested that canonical PI3K/Akt signaling is redundant for myofibroblast transformation and secretion of C4S.

It was further tested whether the mTOR inhibitor AZD8055, which targets both mTORC1 and mTORC2, was required for OGD- and TGFβ1-induced myofibroblast transformation and secretion of C4S. AZD8055 significantly attenuated the phosphorylation of p70S6K (Thr389) and Akt (Ser473) (Fig. 6A, C and D). Fibroblasts treated with 1 μM AZD8055 also robustly inhibited the protein expression of α-SMA and 2H6 (Fig. 6E-G). They also exhibited reduced cellular hypertrophy and immunoreactivity for α-SMA compared with DMSO-treated fibroblasts that received OGD and TGFβ1 stimulation (Fig. 5). These data suggested that mTOR signaling is necessary for myofibroblast transformation and secretion of C4S.
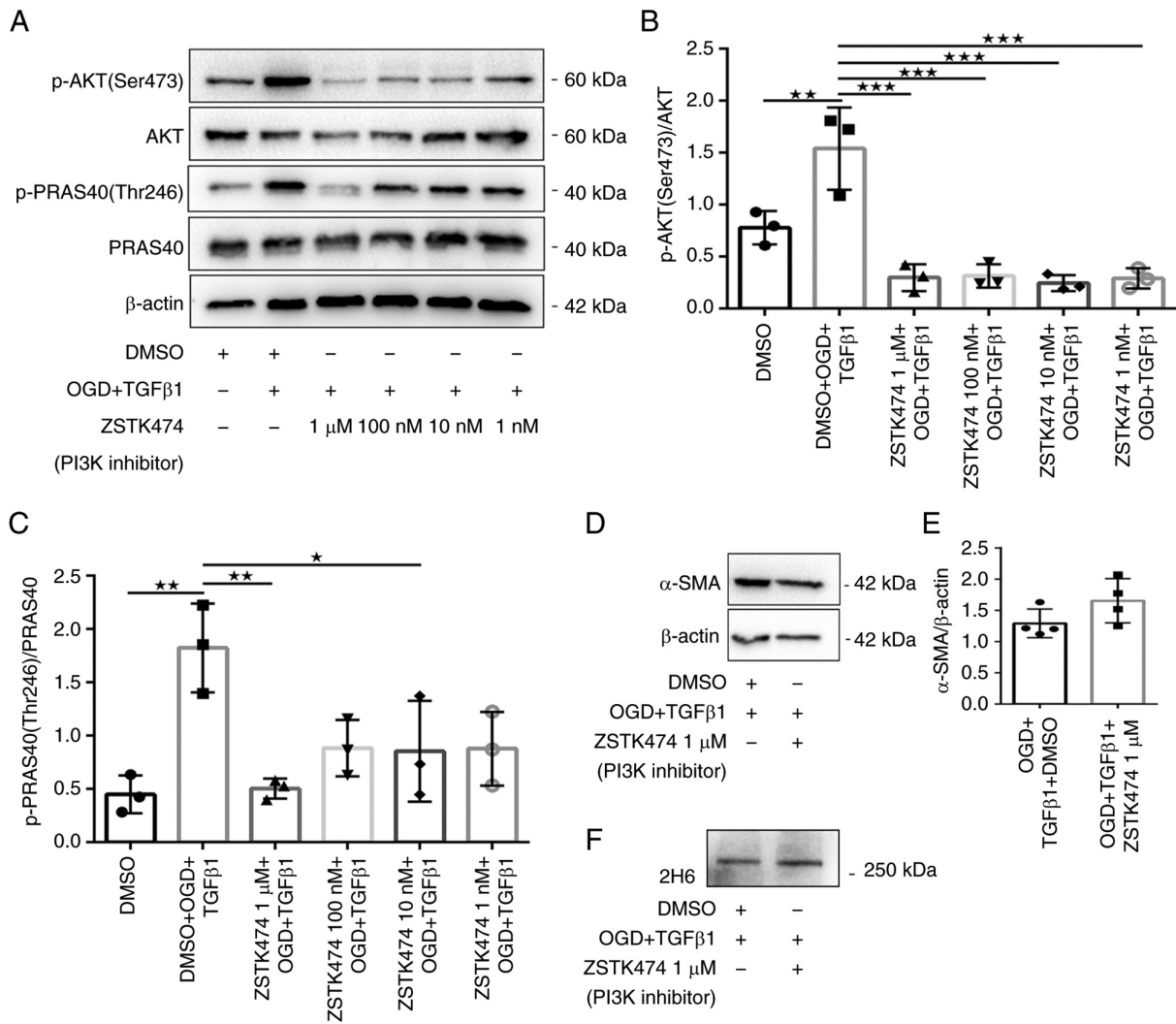
Figure 3. Inhibition of OGD + TGFβ1 induced PI3K/Akt signaling has no effect on the expression of α-SMA or C4S in CFs. CFs were preincubated with DMSO or increasing concentrations of ZSTK474 prior to stimulation with OGD + TGFβ1. (A) Western blotting was used to detect and analyze expression levels of (B) p-AKT(Ser473)/AKT and (C) p-PRAS40(Thr246)/PRAS40. Data are representative of three independent experiments. CFs were preincubated with DMSO or 1 μM ZSTK474 prior to stimulation with OGD + TGFβ1 and the levels of (D and E) α-SMA and (F) 2H6 (using conditioned media) were assessed by western blotting and analyzed. Data are representative of four independent experiments. *P<0.05, **P<0.01 and ***P<0.001. OGD, oxygen-glucose deprivation; CFs, cardiac fibroblasts; α-SMA, α-smooth muscle actin; p-, phosphorylated.

Knockdown of mTORC1 or mTORC2 differentially regulates myofibroblast transformation and secretion of C4S. siRNA was used to silence the expression of Raptor or Rictor in fibroblasts. Western blot analysis demonstrated a significant knockdown of Rictor (mTORC2) or Raptor (mTORC1) in the treatment group (Fig. 7A-B and E-F). OGD- and TGFβ1-induced expression of α-SMA and 2H6 protein levels was maintained in Rictor siRNA knockdown cells (Fig. 7A, C and D). It also exerted no clear effect on cellular hypertrophy or α-SMA immunoreactivity (Fig. 8). By contrast, Raptor siRNA knockdown resulted in significant inhibition of OGD- and TGFβ1-induced protein expression of α-SMA and 2H6 (Fig. 7E, G and H). Cells displayed reduced α-SMA immunoreactivity and cellular hypertrophy (Fig. 8). These data provided evidence that mTORC1 is a key signaling node involved in myofibroblast transformation and secretion of C4S.

The PI3K pathway is considered to be the primary pathway that activates mTORC1. However, neither PI3K nor Akt inhibition affected the downstream signaling of

mTORC1 (Fig. 9A-D). This may suggest another potential PI3K/Akt-independent pathway regulating mTORC1 activation in response to ODG and TGFβ1 stimulation. A previous study reported that inhibition of Erk1/2 activity did not have a significant effect on TGFβ-mediated CSPG expression (15). Another study confirmed that canonical Smad signaling preceded the activation of mTORC1 signaling stimulated by TGFβ1 (13). Therefore, the role of Smad3 in OGD- and TGFβ1-induced myofibroblast transformation and secreted C4S were next investigated.

Knockdown of Smad3 regulates myofibroblast transformation and secretion of C4S. siRNA was used to silence the expression of Smad3 in fibroblasts. Western blot analysis demonstrated a significant knockdown of Smad3 in the treatment group (Fig. 9E-F). OGD- and TGFβ1-induced expression of α-SMA and 2H6 protein levels was significantly reduced in fibroblasts with Smad3 siRNA knockdown (Fig. 9E, G and H). Cells displayed reduced α-SMA immunoreactivity and
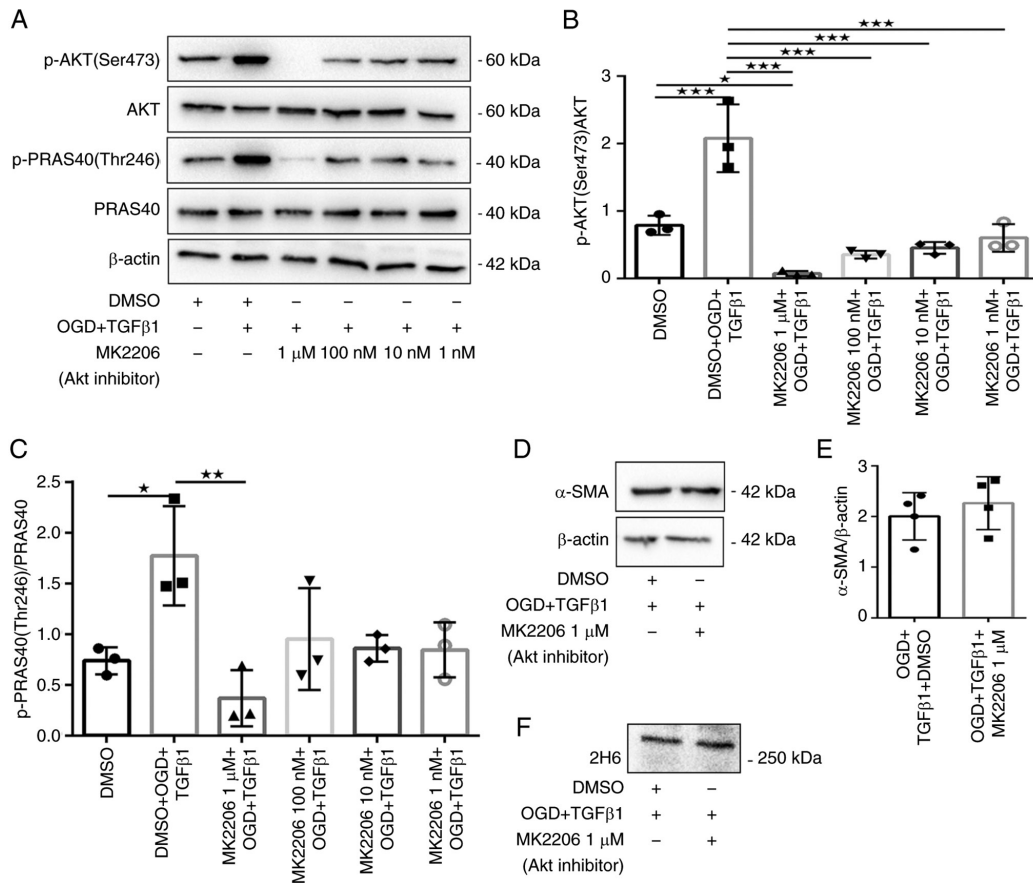
Figure 4. Inhibition of OGD + TGFβ1 induced PI3K/Akt signaling has no effect on the expression of α-SMA or C4S in CFs. CFs were preincubated with DMSO or increasing concentrations of MK2206 prior to stimulation with OGD + TGFβ1. (A) Western blotting was used to detect and analyze expression levels of (B) p-AKT(Ser473)/AKT and (C) p-PRAS40(Thr246)/PRAS40. Data are representative of three independent experiments. CFs were preincubated with DMSO or 1 μM MK2206 prior to stimulation with OGD + TGFβ1 and the levels of (D and E) α-SMA and (F) 2H6 (using conditioned media) were assessed by western blotting and analyses. Data are representative of four independent experiments. *P<0.05, **P<0.01 and ***P<0.001. OGD, oxygen-glucose deprivation; CFs, cardiac fibroblasts; α-SMA, α-smooth muscle actin; p-, phosphorylated.
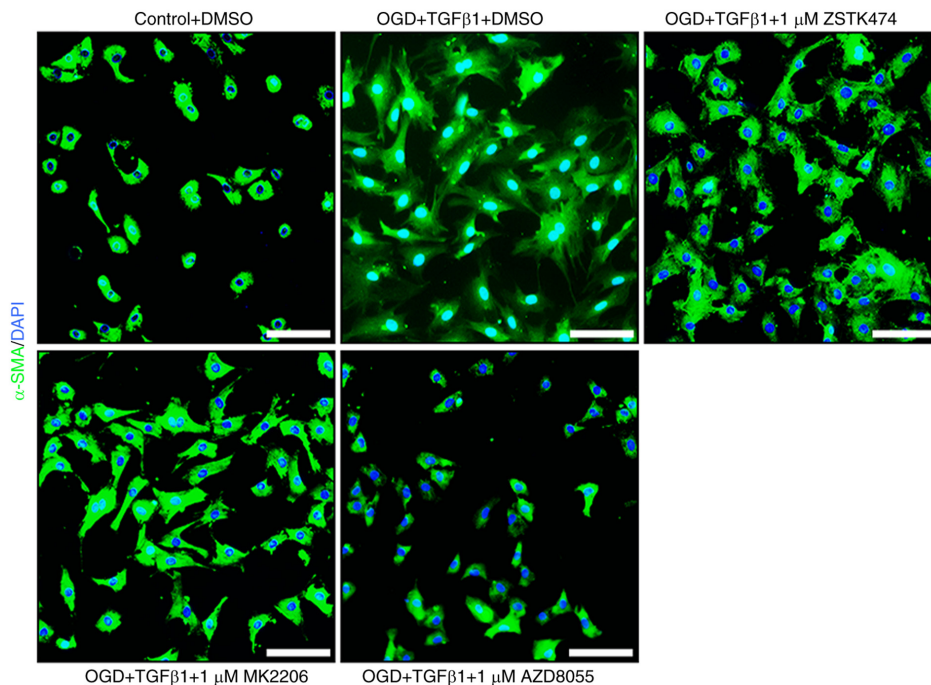

Figure 5. Representative images of CFs treated with DMSO, 1 μM ZSTK474, 1 μM MK2206 or 1 μM AZD8055 prior to stimulation with OGD + TGFβ1. Cells were immunostained for α-SMA (green) and nuclei were stained with DAPI (blue). Scale bar=100 μm. CFs, cardiac fibroblasts; OGD, oxygen-glucose deprivation; α-SMA, α-smooth muscle actin.
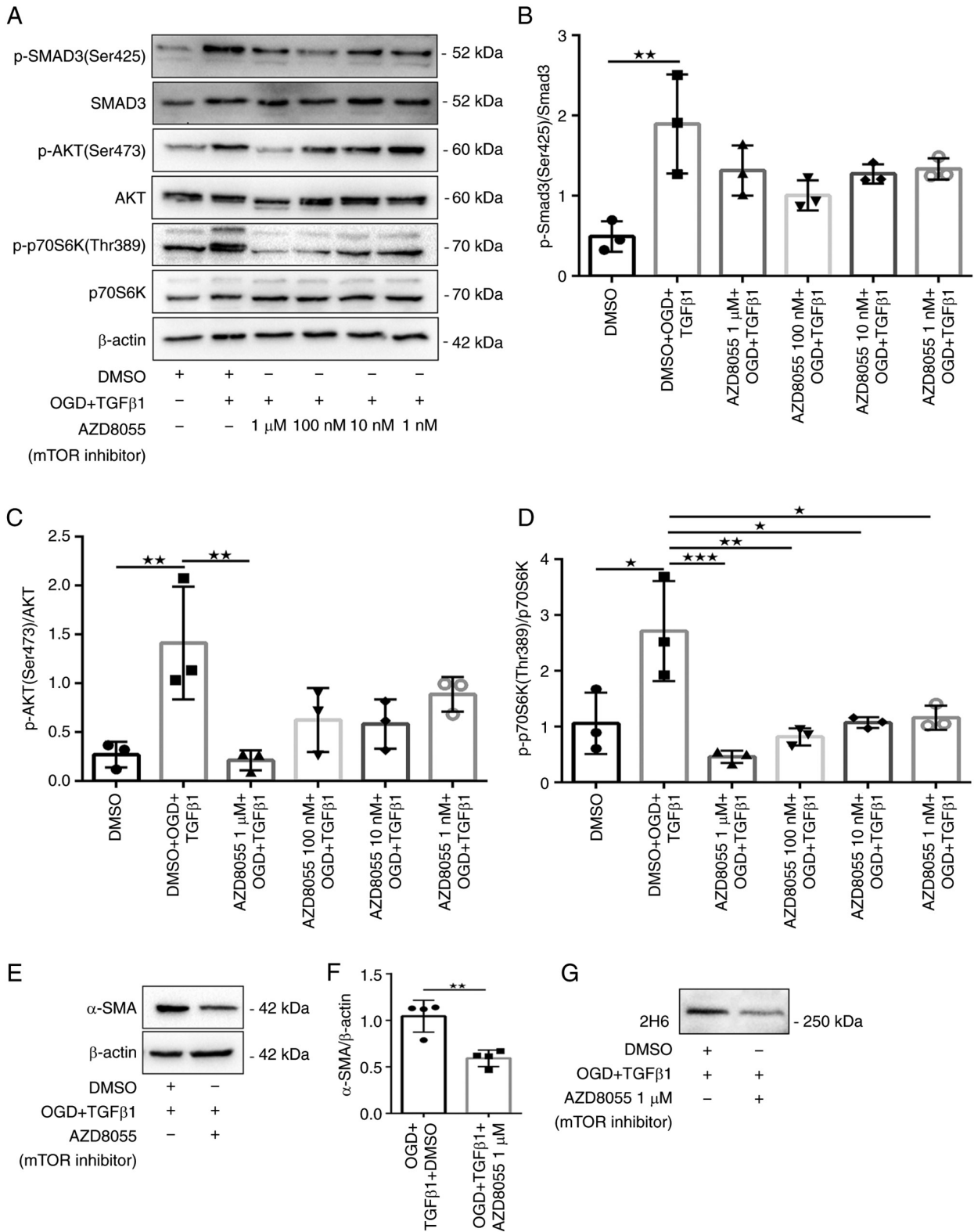
Figure 6. Inhibition of the OGD + TGFβ1 induced mTOR pathway attenuates the expression of α-SMA and C4S in CFs. (CFs were preincubated with DMSO or increasing concentrations of AZD8055 prior to stimulation with OGD + TGFβ1. (A) Western blotting was used to detect and analyze expression levels of (B) p-Smad3(Ser425)/Smad3, (C) p-AKT(Ser473)/AKT and (D) p-p70S6K(Thr389)/p70S6K. Data are representative of three independent experiments. CFs were preincubated with DMSO or 1 μM AZD8055 prior to stimulation with OGD + TGFβ1 and expression levels of (E and F) α-SMA and (G) 2H6 (using conditioned media) assessed by western blotting and analyses. Data are representative of four independent experiments. *P<0.05, **P<0.01 and ***P<0.001. CFs, cardiac fibroblasts; OGD, oxygen-glucose deprivation; α-SMA, α-smooth muscle actin; p-, phosphorylated.

cellular hypertrophy (Fig. 8). These data provided evidence that Smad3 signaling regulates myofibroblast transformation and secretion of C4S.

Myofibroblast transformation and C4S expression may be mediated by cooperation between canonical Smad3 and mTORC1 signaling. Whether Smad is necessary to
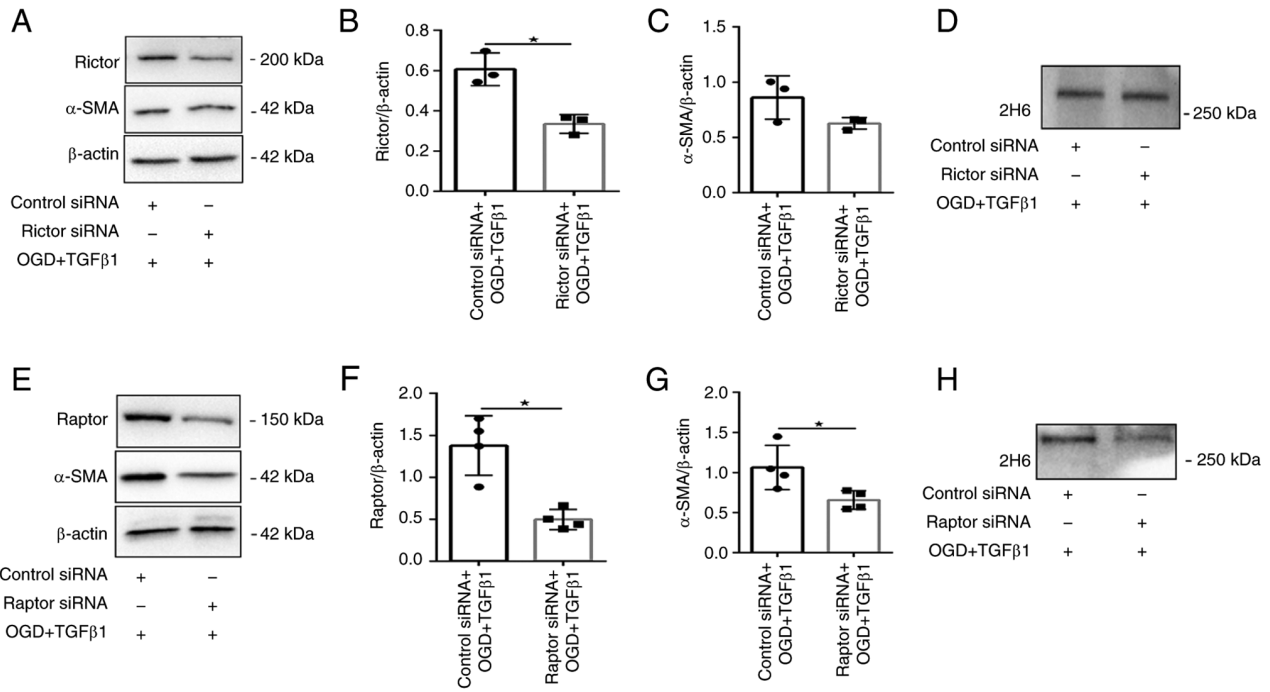
Figure 7. siRNA knockdown of mTORC1 or mTORC2 differentially regulates the expression of α-SMA and 2H6. CFs were preincubated with control siRNA or Rictor siRNA prior to stimulation with OGD + TGFβ1 and expression levels of (A and B) Rictor, (A and C) α-SMA and (D) 2H6 (using conditioned media) were detected by western blotting and analyzed. Data are representative of (A-C) three or (D) four independent experiments. CFs were preincubated with control siRNA or Raptor siRNA prior to stimulation with OGD + TGFβ1 and expression levels of (E and F) Raptor, (E and G) α-SMA and (H) 2H6 (using conditioned media) were detected by western blotting and analyses. Data are representative of four independent experiments. *P<0.05. si, short interfering; α-SMA, α-smooth muscle actin; CFs, cardiac fibroblasts; OGD, oxygen-glucose deprivation.
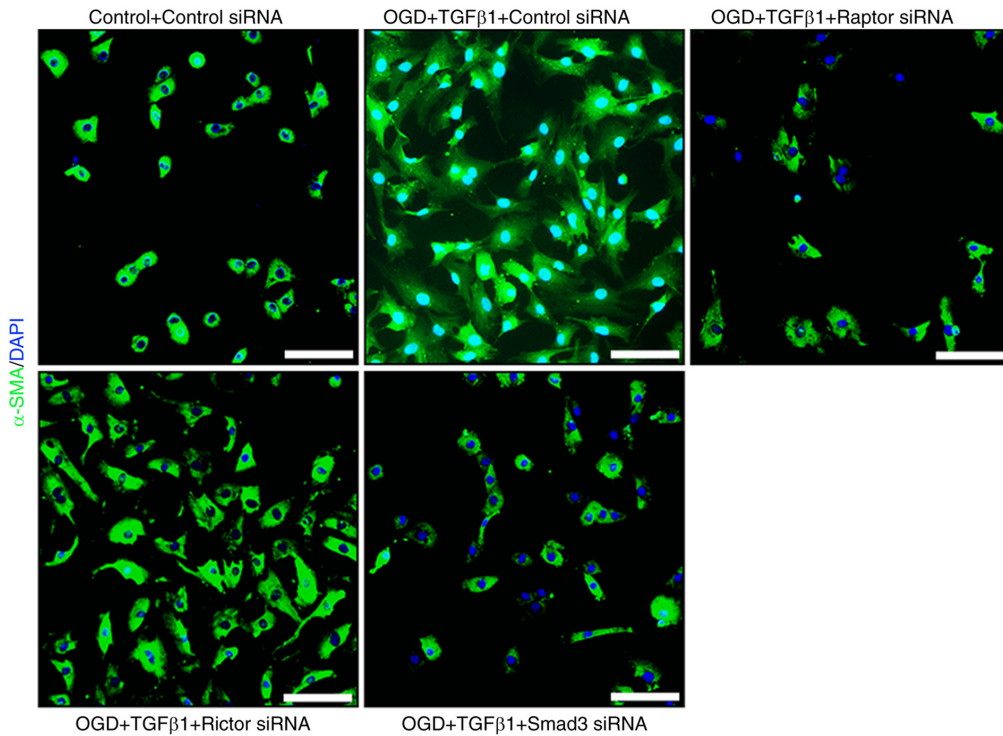

Figure 8. Representative images of CFs treated with control siRNA, Raptor siRNA, Rictor siRNA or Smad3 siRNA prior to stimulation with OGD + TGFβ1. Cells were immunostained for α-SMA (green) and nuclei were stained with DAPI (blue). Scale bar=100 µm. CFs, cardiac fibroblasts; si, short interfering; OGD, oxygen-glucose deprivation; α-SMA, α-smooth muscle actin.

activate mTORC1 was next examined. The data showed that mTORC1-dependent phosphorylation of p70S6K (Thr389)

was significantly reduced in fibroblasts with Smad3 siRNA knockdown, suggesting that activation of mTORC1 is Smad3
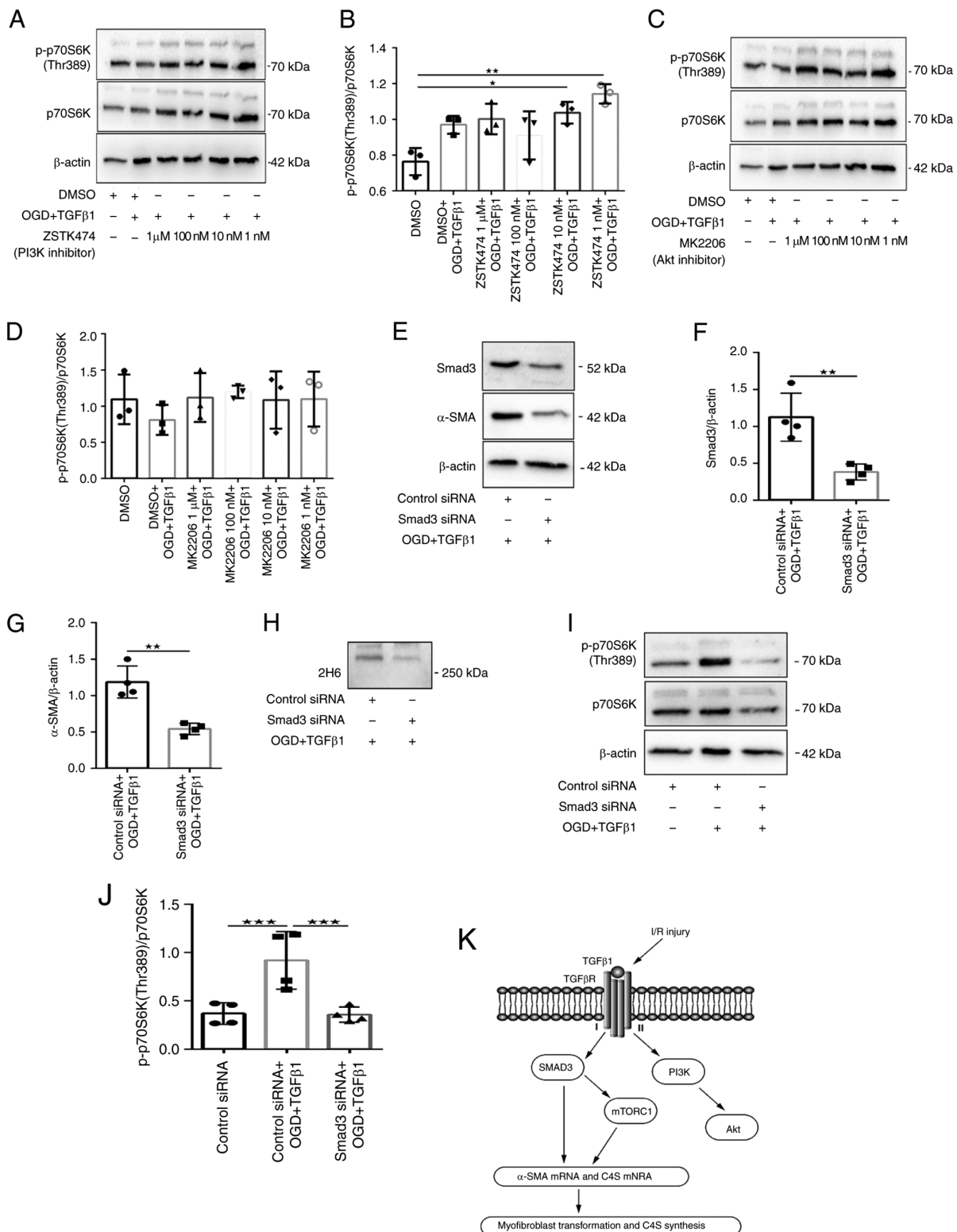
Figure 9. Knockdown of Smad3 reduces the expression of α-SMA and 2H6 and Smad3 is necessary to activate mTORC1. (A and B) CFs were preincubated with DMSO or increasing concentrations of ZSTK474 prior to stimulation with OGD + TGFβ1. Expression levels of specified proteins were detected by western blotting and analyzed. Data are representative of three independent experiments. (C and D) CFs were preincubated with DMSO or increasing concentrations of MK2206 prior to stimulation with OGD + TGFβ1. Expression levels of specified proteins were detected by western blotting and analyses. Data are representative of three independent experiments. CFs were preincubated with control siRNA or Smad3 siRNA prior to stimulation with OGD + TGFβ1. Expression levels of (E and F) Smad3, (E and G) α-SMA and (H) 2H6 (using conditioned media) were detected by western blotting and analyzed. Data are representative of four independent experiments. (I and J) CFs were preincubated with control siRNA or Smad3 siRNA prior to stimulation with OGD+TGFβ1. Expression levels of specified proteins were detected by western blotting and analyses. Data are representative of four independent experiments. (K) Signaling pathways that contribute to myofibroblast transformation and that C4S synthesis. OGD- and TGFβ1 stimulation *in vitro* was used to try to mimic the pathological setting of I/R injury. OGD- and TGFβ1 stimulation induced myofibroblast transformation and that C4S synthesis was Smad3 dependent. mTORC1 was critical for promoting OGD- and TGFβ1 induced myofibroblast transformation and C4S synthesis. This response may be mediated via cooperation between canonical Smad3 and mTORC1 signaling, whereas the upstream canonical PI3K/Akt axis was dispensable. *P<0.05, **P<0.01 and ***P<0.001. α-SMA, α-smooth muscle actin; CFs, cardiac fibroblasts; OGD, oxygen-glucose deprivation; si, short interfering; C4S, chondroitin-4-sulfate; I/R, ischemia and reperfusion.

dependent (Fig. 9I-J). It was also confirmed that the mTOR inhibitor AZD8055 had no significant downregulation of phosphorylation of Smad3 (Ser425) (Fig. 6A-B). These results may indicate that Smad signaling is temporally upstream of mTOR. It was also confirmed that Smad3 knockdown was associated with a significant reduction in the protein expression of α-SMA and 2H6. These data may suggest that OGD and TGFβ1 stimulation induce myofibroblast transformation and secretion of C4S, which may be mediated by cooperation between canonical Smad3 and mTORC1 signaling.

Discussion

The present study revealed that OGD and TGFβ1 stimulation induced fibroblast differentiation into myofibroblasts and C4S synthesis *in vitro*. The data demonstrated that mTORC1 was critical for OGD and TGFβ1 stimulation inducing myofibroblast transformation and C4S expression, whereas the upstream canonical PI3K/Akt axis was dispensable. This response may be mediated via cooperation between canonical Smad3 and mTORC1 signaling.

It is well known that TGFβ1 exerts cardioprotective effects and anti-apoptotic activity in CF under simulated I/R (19). The data from the present study are in accordance with the previous observations (19,20); it was also demonstrated that TGFβ1 partly prevented OGD induced CFs death. Following MI, TGFβ1 was also markedly upregulated and the induced fibroblasts underwent myofibroblast transdifferentiation and ECM protein synthesis (3). It was also found that CFs exposed to OGD and TGFβ1 stimulation displayed visible signs of hypertrophy and robust upregulation of α-SMA mRNA and protein levels compared with the control group. This result suggested fibroblast activation and differentiation into myofibroblasts. The cardiac ECM contains collagens, glycosaminoglycans, glycoproteins and proteoglycans (21). A previous study showed that I/R infarct-derived CSPGs act through protein tyrosine phosphatase receptor σ on sympathetic neurons, leading to persistent postinfarction sympathetic denervation (10,11). Another study demonstrated that excessive CSPG deposition is associated with impaired cardiac function with ischemic HF in animal models and patients (9). The present study investigated the mRNA expression of CSPG protein cores, GAG chain initiation and elongation enzymes and CS sulfatase enzymes. Notably, compared with the control group, only C4st1, the C4S sulfotransferase gene that was increased the 4-sulfation of GAG chains, was highly expressed in the treatment group. It was also confirmed that 2H6, which probes for the major CS component of C4S, was highly expressed in the treatment group compared with the control group. A previous study evaluated TGFβ-induced C4S upregulation in CFs and found that C4S also accumulates in fibrotic regions of the pathologically remodeled LV. It also showed that the relative CS composition remains unchanged between healthy and diseased individuals and C4S was the predominant CS component (5). Another study on CNS injury demonstrates that the GAG chains of CSPGs, especially those with 4-sulfated sugars within the glial scar, serve a major role in inhibiting axonal regeneration (22).

Little is known regarding the molecular mechanisms underlying CSPG expression by CFs following I/R. A previous study confirms TGFβ-Smad3-mediated induction of 4-sulfation as a critical determinant of astrocyte-secreted CSPGs (14). However, another study reported that TGFβ mediated CSPG expression through non-Smad-mediated activation of the PI3K-Akt-mTOR signaling pathway and showed that Smad and MEK1/2 signaling were not required for TGFβ-induced CSPG expression (15). As these two studies reached opposing conclusions, this phenomenon aroused the authors' interest.

The present study found that compared with the control group, Smad3 (Ser425) phosphorylation was strongly upregulated in the treatment group. Previous studies have indicated that Smad3 is a critical mediator of myofibroblast differentiation *in vitro* and is the dominant effector of cardiac fibrosis *in vivo*, but Smad2 is not necessary for this response (23,24). Therefore, Smad3 was knocked down using siRNA in the treatment group and under these conditions, expression of α-SMA and 2H6 was significantly reduced. Smad3 knockdown also reduced α-SMA immunoreactivity and cellular hypertrophy. These data led to the conclusion that knocking down Smad3 to inhibit the reactive phenotype of CFs also reduced C4S synthesis.

In addition to the canonical Smad-mediated signaling pathway, TGFβ can activate numerous Smad-independent signaling pathways. The PI3K-Akt-mTOR signaling pathway regulates diverse biological processes, such as metabolism, cell cycle progression, proliferation, growth, autophagy and protein synthesis. The PI3K-Akt-mTOR signaling pathway has previously been implicated in the transformation of cardiac fibroblasts to a myofibroblast phenotype and ECM synthesis (25,26). In the present study, phosphorylated Akt (Ser473), PRAS40 (Thr246) and p70S6K (Thr389) were also clearly upregulated in the treatment group compared with the control group. These data confirmed that CF treatment with OGD and TGFβ1 induced PI3K/Akt/mTOR signaling activation. A previous study showed that canonical PI3K/Akt signaling has no effect on TGFβ1-induced collagen deposition (13). Thus, the present study further investigated the effect of the PI3K-Akt-mTOR signaling pathway on inducing α-SMA and C4S expression in the treatment group. The present study confirmed that CFs treated with class 1 PI3K or Akt inhibitors (ZSTK474 or MK2206) in the treatment group markedly attenuated Akt signaling but had no effect on the protein expression of α-SMA or 2H6. Fibroblasts retained a reactive phenotype in the presence of 1 μM ZSTK474 or MK2206. This result contrasted with a previous study reporting a role for PI3K in TGFβ1-mediated CSPG synthesis. This may be due to the earlier study using the first-generation PI3K inhibitor LY294002, which can inhibit a variety of other PI3K-related proteins, including mTOR (13). The present study used ZSTK474, which exhibits excellent selectivity for all class 1 PI3K isomers over mTOR.

The present study further demonstrated that an mTOR inhibitor (AZD8055) attenuated the phosphorylation of p70S6K (Thr389) and Akt (Ser473) and significantly reduced the protein expression of α-SMA and 2H6 in the treatment group. mTOR inhibition also reduced cellular hypertrophy and immunoreactivity. This suggested that mTOR serves a key role in myofibroblast transformation and the expression of C4S. The present study further investigated the relative contributions of mTORC1 and mTORC2 by knocking down either Raptor or Rictor using siRNA. The data suggested that

mTORC1 mediated the expression of α-SMA and C4S in CFs induced by OGD and TGFβ1 stimulation.

Notably, the results suggested that neither PI3K nor Akt inhibition affected mTORC1 downstream signaling expression in the treatment group. A previous study showed that in the lung fibroblast response to TGFβ1 stimulation, maximal phosphorylation of mTORC1 substrates is consistently observed at least 10 h before maximal phosphorylation of Akt (13). This may suggest another potential PI3K/Akt-independent pathway regulating mTORC1 activation. The present study confirmed that Smad3 is necessary for the activation of mTORC1 (13). It also examined whether this reflection affected the expression of α-SMA and C4S in the treatment group and reached a similar conclusion: Targeted knockdown of Smad3 with siRNA in the treatment group attenuated mTORC1-dependent phosphorylation of p70S6K and significantly reduced the protein expression of α-SMA and 2H6. In addition, it reduced cellular hypertrophy. The present study also demonstrated that AZD8055 had no effect on the phosphorylation of Smad3 (Ser425). This indicated that Smad3 preceded the activation of mTORC1 and that the activation of mTORC1 was Smad3-dependent. These data may indicate that OGD and TGFβ1 stimulation induced myofibroblast transformation and that C4S expression is mediated by cooperation between canonical Smad3 and mTORC1 signaling.

There are some limitations to the present study. First, due to limited funding, only a few PI3K/Akt/mTOR pathway targets were selected to verify the hypothesis and no rescue experiments for gene overexpression or follow-up experiments were performed. Second, evidence from *in vivo* experiments was lack and others should further verify the findings using *in vivo* experiments.

In conclusion, the present study presented evidence that mTORC1 was critical for promoting ODG- and TGFβ1-induced expression of α-SMA and C4S, whereas the upstream canonical PI3K/Akt axis was dispensable. This response may be mediated by cooperation between canonical Smad3 and mTORC1 signaling. Although digesting CSPG GAG chains with the bacterial enzyme chondroitinase ABC (ChABC) or rhASB has been shown to promote axonal extension in the CNS (22,27), ChABC has failed to reach clinical trials. Therefore, the present study tried to link the synthesis of C4S with the transdifferentiation of cardiac fibroblasts. These observations suggested that inhibiting myofibroblast differentiation may reduce the expression of C4S. This may provide additional insight into the regeneration of sympathetic nerves and the reduction of fibrosis after MI at the cellular level.

Acknowledgements

Not applicable.

Availability of data and materials

The datasets used and/or analyzed during the current study are available from the corresponding author on reasonable request.

Authors' contributions

CL and ZZ contributed to the conception and design of the present study. CL performed the experiments, collected the data and performed statistical analysis with the help of YP, YZ, WK, YL and YH. CL drafted the manuscript, which was corrected and revised by ZZ. ZZ and YP confirm the authenticity of all the raw data. All authors read and approved the final manuscript.

Ethics approval and consent to participate

All experimental procedures were performed in accordance with the Guide for the Care and Use of Laboratory Animals published by the National Research Council and were approved by the Animal Care Committee of the Gansu University of Chinese Medicine (approval number 2019-212).

Patient consent for publication

Not applicable.

Competing interests

The authors declare that they have no competing interests.

References

1. Wu Y, Liu H and Wang X: Cardioprotection of pharmacological postconditioning on myocardial ischemia/reperfusion injury. Life Sci 264: 118628, 2021.
2. Lai TC, Lee TL, Chang YC, Chen YC, Lin SR, Lin SW, Pu CM, Tsai JS and Chen YL: MicroRNA-221/222 mediates ADSC-Exosome-Induced cardioprotection against ischemia/reperfusion by targeting PUMA and ETS-1. Front Cell Dev Biol 8: 569150, 2020.
3. Chen W and Frangogiannis NG: Fibroblasts in post-infarction inflammation and cardiac repair. Biochim Biophys Acta 1833: 945-953, 2013.
4. Molkentin JD, Bugg D, Ghearing N, Dorn LE, Kim P, Sargent MA, Gunaje J, Otsu K and Davis J: Fibroblast-specific genetic manipulation of p38 mitogen-activated protein kinase in vivo reveals its central regulatory role in fibrosis. Circulation 136: 549-561, 2017.
5. Zhao RR, Ackers-Johnson M, Stenzig J, Chen C, Ding T, Zhou Y, Wang P, Ng SL, Li PY, Teo G, *et al*: Targeting chondroitin sulfate glycosaminoglycans to treat cardiac fibrosis in pathological remodeling. Circulation 137: 2497-2513, 2018.
6. Chelini G, Pantazopoulos H, Durning P and Berretta S: The tetrapartite synapse: A key concept in the pathophysiology of schizophrenia. Eur Psychiatry 50: 60-69, 2018.
7. Hayes AJ and Melrose J: Neural tissue homeostasis and repair is regulated via CS and DS proteoglycan motifs. Front Cell Dev Biol 9: 696640, 2021.
8. Kai Y, Tomoda K, Yoneyama H, Kitabatake M, Nakamura A, Ito T, Yoshikawa M and Kimura H: Silencing of carbohydrate sulfotransferase 15 hinders murine pulmonary fibrosis development. Mol Ther Nucleic Acids 6: 163-172, 2017.
9. Barallobre-Barreiro J, Radovits T, Fava M, Mayr U, Lin WY, Ermolaeva E, Martínez-López D, Lindberg EL, Duregotti E, Daróczi L, *et al*: Extracellular matrix in heart failure: Role of ADAMTS5 in proteoglycan remodeling. Circulation 144: 2021-2034, 2021.
10. Gardner RT and Habecker BA: Infarct-derived chondroitin sulfate proteoglycans prevent sympathetic reinnervation after cardiac ischemia-reperfusion injury. J Neurosci 33: 7175-7183, 2013.
11. Gardner RT, Wang L, Lang BT, Cregg JM, Dunbar CL, Woodward WR, Silver J, Ripplinger CM and Habecker BA: Targeting protein tyrosine phosphatase sigma after myocardial infarction restores cardiac sympathetic innervation and prevents arrhythmias. Nat Commun 6: 6235, 2015.

12. Miyata S and Kitagawa H: Chondroitin sulfate and neuronal disorders. Front Biosci (Landmark Ed) 21: 1330-1340, 2016.
13. Woodcock HV, Eley JD, Guillotin D, Platé M, Nanthakumar CB, Martufi M, Peace S, Joberty G, Poeckel D, Good RB, *et al*: The mTORC1/4E-BP1 axis represents a critical signaling node during fibrogenesis. Nat Commun 10: 6, 2019.
14. Susarla BT, Laing ED, Yu P, Katagiri Y, Geller HM and Symes AJ: Smad proteins differentially regulate transforming growth-β-mediated induction of chondroitin sulfate proteoglycans. J Neurochem 119: 868-878, 2011.
15. Jahan N and Hannila SS: Transforming growth factor β-induced expression of chondroitin sulfate proteoglycans is mediated through non-Smad signaling pathways. Exp Neurol 263: 372-384, 2015.
16. Tian K, Liu Z, Wang J, Xu S, You T and Liu P: Sirtuin-6 inhibits cardiac fibroblasts differentiation into myofibroblasts via inactivation of nuclear factor kappaB signaling. Transl Res 165: 374-386, 2015.
17. Ryou MG and Mallet RT: An in vitro oxygen-glucose deprivation model for studying ischemia-reperfusion injury of neuronal cells. Methods Mol Biol 1717: 229-235, 2018.
18. Livak KJ and Schmittgen TD: Analysis of relative gene expression data using real-time quantitative PCR and the 2(-Delta Delta C(T)) method. Methods 25: 402-408, 2001.
19. Olivares-Silva F, Espitia-Corredor J, Letelier A, Vivar R, Parra-Flores P, Olmedo I, Montenegro J, Pardo-Jiménez V and Díaz-Araya G: TGF-β1 decreases CHOP expression and prevents cardiac fibroblast apoptosis induced by endoplasmic reticulum stress. Toxicology In vitro 70: 105041, 2021.
20. Vivar R, Humeres C, Ayala P, Olmedo I, Catalán M, García L, Lavandero S and Díaz-Araya G: TGF-β1 prevents simulated ischemia/reperfusion-induced cardiac fibroblast apoptosis by activation of both canonical and non-canonical signaling pathways. Biochim Biophys Acta 1832: 754-762, 2013.
21. Frangogiannis NG: Cardiac fibrosis: Cell biological mechanisms, molecular pathways and therapeutic opportunities. Mol Aspects Med 65: 70-99, 2019.
22. Pearson CS, Mencio CP, Barber AC, Martin KR and Geller HM: Identification of a critical sulfation in chondroitin that inhibits axonal regeneration. ELife 7: e37139, 2018.
23. Khalil H, Kanisicak O, Prasad V, Correll RN, Fu X, Schips T, Vagnozzi RJ, Liu R, Huynh T, Lee SJ, *et al*: Fibroblast-specific TGF-β-Smad2/3 signaling underlies cardiac fibrosis. J Clin Invest 127: 3770-3783, 2017.
24. Huang S, Chen B, Su Y, Alex L, Humeres C, Shinde AV, Conway SJ and Frangogiannis NG: Distinct roles of myofibroblast-specific Smad2 and Smad3 signaling in repair and remodeling of the infarcted heart. J Mol Cell Cardiol 132: 84-97, 2019.
25. Zhang J, Fan G, Zhao H, Wang Z, Li F, Zhang P, Zhang J, Wang X and Wang W: Targeted inhibition of focal adhesion kinase attenuates cardiac fibrosis and preserves heart function in adverse cardiac remodeling. Sci Rep 7: 43146, 2017.
26. Bradley JM, Spaletra P, Li Z, Sharp TE III, Goodchild TT, Corral LG, Fung L, Chan KW, Sullivan RW, Swindlehurst CA and Lefer DJ: A novel fibroblast activation inhibitor attenuates left ventricular remodeling and preserves cardiac function in heart failure. Am J Physiol Heart Circ Physiol 315: H563-H570, 2018.
27. Kwok JC, Heller JP, Zhao RR and Fawcett JW: Targeting inhibitory chondroitin sulphate proteoglycans to promote plasticity after injury. Methods Mol Biol 1162: 127-138, 2014.